Stem Cell Reports, Volume *16*

Supplemental Information

NOTCH-mediated *ex vivo* expansion of human hematopoietic stem and progenitor cells by culture under hypoxia

Daisuke Araki, Jian Fei Fu, Heather Huntsman, Stefan Cordes, Fayaz Seifuddin, Luigi J. Alvarado, Patali S. Cheruku, Ayla Cash, Javier Traba, Yuesheng Li, Mehdi Pirooznia, Richard H. Smith, and Andre Larochelle

Supplemental Material for
NOTCH-Mediated *Ex Vivo* Expansion
of Human Hematopoietic Stem and Progenitor Cells
by Culture Under Hypoxia

Daisuke Araki[†1], Jian Fei Fu[†§1], Heather Huntsman[†1], Stefan Cordes[2], Fayaz Seifuddin[3], Luigi J. Alvarado[1], Patali S. Cheruku[1], Ayla Cash[1], Javier Traba[4], Yuesheng Li[5], Mehdi Pirooznia[3], Richard H. Smith[1], Andre Larochelle[*1]

Affiliations:

(1) Cellular and Molecular Therapeutics Branch, National Heart, Lung and Blood Institute (NHLBI), National Institutes of Health (NIH), Bethesda, MD 20892, USA
(2) Translational Stem Cell Biology Branch, NHLBI, NIH, Bethesda, MD 20892, USA
(3) Bioinformatics and Computational Biology Laboratory, NHLBI, NIH, Bethesda, MD 20892, USA
(4) Cardiovascular Branch, NHLBI, NIH, Bethesda, MD 20892, USA
(5) DNA Sequencing and Genomics Core Facility, NHLBI, NIH, Bethesda, MD 20892, USA

Author list footnotes:

[†]These authors contributed equally

[§]Current address: Department of hematology, Tongji Hospital Affiliated to Tongji University, China

* Corresponding author: Andre Larochelle, M.D. Ph.D., National Heart, Lung and Blood Institute, National Institutes of Health, 9000 Rockville Pike, Bethesda, MD 20892, USA

 (301) 451-7139  larochea@nhlbi.nih.gov  (301) 496-8396

This PDF file includes:

- Supplemental Methods
- Supplemental Figures
  - **Figure S1** | Concurrent activation of NOTCH and hypoxia pathways in human CD34+ cells has minimal impact on cell survival or lineage differentiation. Associated with Figure 1A.
  - **Figure S2** | Transcriptomic analysis of CD34+ cells treated with DXI in normoxic or hypoxic cultures. Associated with Figure 2A, and Tables S1 and S2.
  - **Figure S3** | Hypoxia does not affect signaling mediated by the intracellular domain of NOTCH2. Associated with Figure 2, C-F.
  - **Figure S4** | Single cell RNA sequencing analysis of CD34+ cells treated with optimized DXI densities under normoxic or hypoxic conditions. Associated with Figure 4, and Tables S3 and S4.
  - **Figure S5** | Downregulation of ER stress response gene expression by hypoxia during DXI-mediated expansion of human long-term repopulating HSCs. Associated with Figure 4D.

The accompanying Excel file includes all Supplemental Tables:

- **Table S1** | Complete list of differentially expressed genes in human CD34+ cells analyzed by bulk RNA sequencing. Associated with Figure S2C.
- **Table S2** | Complete list of genes in the leading edge subsets from Gene Set Enrichment Analysis (GSEA) on custom pathway in bulk RNA sequencing. Associated with Figures 2A, 3E, 3F, and S2D.
- **Table S3** | Complete list of differentially expressed genes within the HSC cluster of human CD34+ cells analyzed by single cell RNA sequencing using the Wilcoxon rank sum test. Associated with Figures 4D and S4C.
- **Table S4** | Complete list of differentially expressed genes within the HSC cluster of human CD34+ cells analyzed by single cell RNA sequencing using the DESeq2 test. Associated with Figures 4D and S4D.
- **Table S5** | Complete list of up- and down-regulated GO molecular function terms within the HSC cluster of human CD34+ cells analyzed by single cell RNA sequencing. Associated with Figure 4E.

Supplemental Methods

Isolation of human CD34+ HSPCs

Human CD34+ HSPCs were obtained from healthy male and female volunteers (ages 18-60) after informed consent in accordance with the Declaration of Helsinki, under an Institutional Review Board-approved clinical protocol (NCT00001529). Peripheral blood mobilization of HSPCs was induced via subcutaneous injection of 10 ug/kg G-CSF (Filgrastim, Amgen) for 5 days followed by leukapheresis using a Cobe Spectra Apheresis System (Terumo BCT). The mononuclear cell concentrates were enriched in CD34+ HSPCs using a CliniMACS Plus instrument (Miltenyi Biotec) and cryopreserved prior to use.

Cell culture design and consideration

To investigate whether hypoxia can facilitate superior *ex vivo* expansion of human HSPCs than normoxia in the presence of DXI, a total of 1 x 10^5 human MPB CD34+ cells were cultured for 21 days under normoxic (21% O_2) or hypoxic (1-2% O_2) conditions in vessels coated with fibronectin alone or combined with increasing concentrations of DXI (2.5, 5, 10 and 20 µg/mL). Media was changed every 3 days, and cells were maintained at no more than 90% confluency. We chose this extended 21-day culture period for direct comparison with previous studies utilizing DXI for *ex vivo* expansion of human HSPCs (Delaney et al., 2010; Delaney et al., 2005). Importantly, strict hypoxic conditions were maintained at all times; hypoxic chambers and gloveboxes were used for culture and medium changes, all reagents were equilibrated to hypoxia prior to use, and oxygen tensions (1-2%) previously shown to maintain and expand repopulating HSPCs (Cipolleschi et al., 1993; Danet et al., 2003) were selected for these studies. The anticipated metabolic shift induced by strict hypoxia was confirmed using a Seahorse extracellular flux analyzer. After expansion, cells were counted and characterized by a series of in-vitro and in-vivo functional assays.

Colony-forming unit (CFU) assay

Uncultured CD34+ cells or the 21-day *ex vivo* expanded cells were plated into 35 mm non-tissue culture treated dishes in 1 mL of MethoCult™ H4435 Enriched (STEMCELL Technologies) at a concentration of 1500 cells/mL for all conditions. After 12-14 days in culture, colonies were counted and scored based on morphological features using an EVOS XL Core transmitted light microscope (Thermo Fisher Scientific).

Cell surface phenotypic analysis

Cell surface phenotypes were assessed using a combination of the following antibody pane (all from Becton Dickinson Biosciences [BD], unless stated otherwise): PE- or Alexaflour700-anti-CD34 (555822 or 561440), APC-anti-CD38 (555462), PE-Cy7-anti-CD90 (561558), APC-H7-anti-CD45RA (561212), PE-anti-CD45 (555483), APC-anti-CD13 (555394), APC-anti-CD14 (561383), Alexaflour700-anti-CD71 (563769), PE-Cy5-anti-CD41 (BioLegend, 303708), PE-Cy7-anti-CD20 (560735) and APC-Cy7-anti-CD3 (557757). All stained cells were analyzed using an LSR II Fortessa flow cytometer (BD).

Apoptosis assay

Cellular survival and apoptosis were quantified using Annexin V Apoptosis Detection kit (Thermo Fisher Scientific, 88-8006-74) according to the manufacturer's instructions. After 24 hours or 21 days of incubation, cultured HSPCs were collected and incubated with human Fc Block™ (BD, 564219) for 10 minutes at room temperature. Then, cells were stained with PE-anti-CD34, APC-anti-CD38, PE-Cy7-anti-CD90 and APC-H7-anti-CD45RA on ice for 15 minutes. After washing in 1X binding buffer, cells were stained using eFlour450-Annexin V for 15 minutes at room temperature. After cells were washed and resuspended in 1X binding buffer, 7-AAD viability staining solution (Thermo Fisher Scientific, 00-6993) was added, and stained cells were immediately analyzed using an LSR II Fortessa flow cytometer (BD).

Protein aggregation assay

Aggregated proteins were quantified using ProteoStat staining (Enzo Life Sciences, ENZ-51023-KP050). The proteosome inhibitor MG-132 at 100 nM was used to induce protein aggregate

formation (positive control). After 24 hours of incubation, cultured HSPCs were collected and incubated with human Fc Block™ (BD, 564219) for 10 minutes at room temperature. Then, cells were stained with Alexaflour700-anti-CD34, APC-anti-CD38, PE-Cy7-anti-CD90 and APC-H7-anti-CD45RA on ice for 30 minutes. After washing, cells were fixed in Cytofix/Cytoperm Fixation and Permeabilization Solution (BD, 554714) on ice for 30 minutes. After washing, fixed cells were stained with the ProteoStat dye (1:5000) dilution in Permeabilization Solution for 30 minutes at room temperature. After washing with FACS buffer, cells were immediately analyzed using an LSR II Fortessa flow cytometer (BD).

Reactive oxygen species quantification

Reactive oxygen species was quantified using CellROX Green reagent following the manufacturer's instructions (Thermo Fisher Scientific, ref. C10444). Menadione at 50 µM for one hour was used to induce ROS signals (positive control). After 24 hours of incubation, cultured HSPCs were stained with CellROX Green dye at 5 µM in complete medium for 30 minutes at 37°C. After removing medium and washing 3 times in PBS, cells were stained with Alexaflour700-anti-CD34, APC-anti-CD38, PE-Cy7 anti-CD90, APC-H7-anti-CD45RA on ice for 15 minutes. After washing with FACS buffer, cells were immediately analyzed using an LSR II Fortessa flow cytometer (BD).

Assessment of human cell engraftment in NSG mice

Levels of human cell engraftment were assessed ≥ 4 months after transplantation. Briefly, tibiae, femurs, and pelvises were harvested from individual mice and bone marrow was flushed from each bone into 2 ml of X-Vivo using an insulin syringe with a 29-gauge needle. Samples were then centrifuged at 1200 rpm for 10 minutes. Red blood cells were lysed by a 5-10 minute incubation at room temperature with ACK lysis buffer (Quality Biological) and the remaining cells were collected by centrifugation at 1200 rpm for 10 minutes. Cells were stained for 30 minutes on ice with the following antibody panel: PE-anti-CD45, PE-Cy7-anti-CD20 and PE-CD13 PE and analyzed on a LSR II Fortessa flow cytometer (BD).

The frequency of LTR-HSCs was determined by an LDA, as previously reported (Hu and Smyth, 2009). The HSC frequency was calculated using ELDA software (http://bioinf.wehi.edu.au/software/elda/) and plotted using limdil function in satmod package within the RStudio IDE. Human engraftment was defined as CD45+ cells ≥ 0.1%.

Seahorse extracellular flux assay

The extracellular acidification rate (ECAR) or oxygen consumption rate (OCR) of human mobilized peripheral blood $CD34^+$ cells was determined using a Seahorse XF Extracellular Flux Analyzer (Agilent Technologies). A volume of 200 µL XF Calibrant buffer (Seahorse Bioscience) was added into the wells of a Seahorse Bioscience 96-well utility plate and, after an overnight incubation at 37°C, the plate was coated with Cell-Tak solution (Corning) at room temperature for 1 hour. *Ex vivo* expanded $CD34^+$ cells were resuspended with assay medium, and cell number was determined using a Cellometer Auto 2000 Cell Viability Counter (Nexcelom Bioscience). A total of 400000-500000 *ex vivo* cultured $CD34^+$ cells were plated per well and the plates were centrifuged for 10 min at 1000g. Glucose (Sigma), oligomycin (Sigma) and 2-DG (Sigma) solution, or oligomycin, FCCP (Sigma) and rotenone (Sigma) solutions were sequentially added into the wells of the utility plate for ECAR or OCR analysis. The utility plate with the loaded sensor cartridge was placed on the instrument tray for calibration. To evaluate ECAR or OCR of $CD34^+$ cells, when prompted, the calibration plate was replaced with the cell culture microplate, and the 'Start' button was pressed.

Plasmid Construction

HIF-1α P402A/P564A construct has previously been described (Yan et al., 2007). HIF-1α P402A/P564A-expressing SIN-HIV1 vector plasmid was prepared by digestion-ligation subcloning technique using HA-HIFalpha P402A/P564A-pcDNA3 plasmid (Addgene plasmid #18955).

Lentiviral vector preparation

The χHIV vector was prepared by four plasmid cotransfections of 293T cells by χHIV Gag/Pol plasmid, HIV1 Rev/Tat plasmid, VSV-G envelope plasmid, and HIF-1α P402A/P564A-expressing SIN-HIV1 vector plasmid, as previously described (Uchida et al., 2011). In all vectors, the transgenes were driven by an EF1α promoter. Biological titers of lentiviral vectors were measured in human CD34+ cells.

Transduction of human CD34+ HSPCs

Human $CD34^+$ cells were cultured overnight on RetroNectin-coated (Takara) plates in StemSpan media (STEMCELL Technologies) supplemented with 100 ng/ml each human cytokine FLT3, SCF and TPO (PeproTech) and 1% human albumin, and transduced with HIF-1α P402A/P564A expressing lentiviral vectors in the presence of 4 μg/ml protamine sulfate (Sigma).

Quantitative Reverse transcription PCR

RNA was extracted using the RNeasy Plus Mini Kit (Qiagen) according to the manufacturer's instructions. The genomic DNA elimination columns contained in the kit were used to eliminate possible DNA contamination during the extraction. Quantitative reverse transcription (RT) and real-time PCR (qRT-PCR) were done using TaqMan™ RNA-to_Ct 1-Step kit (AB 4392938) on BioRad CFX 96 Real-time systems with the following TaqMan™ probes and primers purchased from Thermo Fisher Scientific; ACTB-VIC (Hs01060665_g1), HES1-FAM (Hs00172878_m1), HIF1A-FAM (Mm00468869_m1), HSP90AA1-FAM (Hs00743767_sH), HSPH1-FAM (Hs00971475_m1), HSPA1A-FAM (Hs00359163_s1), HSPB1-FAM (Hs00356629_g1) and HSPE1-FAM (Hs01654720_g1). Reactions were multiplexed to include primers and probes for the gene of interest and a housekeeping gene (beta-actin).

Western blot

Mutant HIF-1α-overexpressing CD34+ cells were washed with PBS three times and collected with Pierce IP Lysis Buffer (Thermo Fisher Scientific) and Roche cOmplete™ EDTA-free Protease Inhibitor Cocktail (Sigma). Protein concentration was determined using the Qubit assay (Thermo Fisher Scientific). Equal amounts of proteins were electrophoresed via NuPAGE™ 4 to 12% Bis-

Tris 1.5 mm Mini Protein Gel 10% (Thermo Fisher Scientific) with MES SDS running buffer (Thermo Fisher Scientific) combined with NuPAGE antioxidant (Thermo Fisher Scientific). Gel bands were then electro-transferred to PVDF nitrocellulose membranes (Thermo Fisher Scientific). Membranes were blocked with Blotto, 5% non-fat dry milk (Santa Cruz Biotechnology) for 1 hour at room temperature, followed by incubation with 1:1000 primary rabbit anti-HA-tag antibody (Cell Signaling) overnight at 4°C. Blots were washed three times with PBS Tween 20 Buffer (PBS-T) (Thermo Fisher Scientific) and incubated with 1:1000 goat anti-rabbit HRP-linked secondary antibody (Cell Signaling) for 60 minutes at room temperature. Following three washes with PBS-T to remove excess antibody, membranes were soaked for 3 minutes in SuperSignal™ West Dura Extended Duration Substrate (Thermo Fisher Scientific) and then analyzed via chemiluminescence using a LAS-4000 (Fujifilm Life Science).

Bulk RNA sequencing and data analysis

Human CD34+ cells from 6 different healthy donors were cultured in the presence of cytokines (SCF, FLT3 and TPO) in vessels coated with DXI at 10 µg/mL in normoxia and 5 µg/mL in hypoxia for 24 hours. Cells were subsequently harvested, and RNA was extracted using the RNeasy Plus Mini Kit (Qiagen) according to the manufacturer's instructions. The genomic DNA elimination columns contained in the kit were used to eliminate possible DNA contamination during the extraction.

The sequencing libraries were constructed from 10 pg–10 ng of total RNA using the Takara Bio USA's SMART-Seq V4 Ultra Low Input RNA Kit for Sequencing (Cat # 634888) following the manufacturer's instructions. Full-length cDNA synthesis was performed using oligo-dT and SMART oligos, and the Illumina sequencing adaptors and barcodes incorporated into the final library by PCR. The fragment size of the RNAseq libraries was verified using the Agilent 2100 Bioanalyzer (Agilent) and the concentrations determined using the Qubit instrument (Thermo Fisher Scientific). The libraries were loaded onto the Illumina HiSeq 3000 machine (Illumina) for

paired end 75 bp read sequencing and generated about 50 M reads per sample. The fastq files were generated using the bcl2fastq software (Illumina) for further analysis.

Rigorous quality controls of paired-end reads were assessed using FastQC tools (Bioinformatics, 2015; QUBES, 2015). Reads were aligned to the reference genome using the latest version of HISAT2 (Kim et al., 2019), which is a splice-aware aligner that sequentially aligns reads to the known transcriptome and genome. FeatureCounts (Liao et al., 2014) was used for gene level abundance estimation using the GENCODE (v25) (Harrow et al., 2012) comprehensive gene annotations. Principal component analysis (PCA) was used to assess outlier samples. Genes were kept in the analysis if they had raw read counts $>$ 5 in at least four samples (for each pairwise comparison performed in the differential expression analysis).

Differential expression analysis comparing an experimental condition (CD34+ cells exposed to 5 µg/mL DXI in hypoxia) versus control (CD34+ cells exposed to 10 µg/mL DXI in normoxia) at the gene levels of summarization were then carried out using open source Limma R package (Smyth G.K., 2005). Limma-voom (Law et al., 2014; Ritchie et al., 2015) was employed to implement a gene-wise linear modelling which processes the read counts into $\log_2$ counts per million (logCPM) with associated precision weights. The $\log_2$CPM values were normalized between samples using trimmed mean of M-values (TMM) (Robinson and Oshlack, 2010). We adjusted the differential expression analysis by using a covariate indicating paired samples from subjects following the experimental design. We adjusted for multiple testing by reporting the FDR values for each feature (Madar and Batista, 2016). Features with $\log_2$ fold change > 1.5 or < -1.5 and q-value $<$ 5% were declared as genome-wide significant.

We used GSEA v4.1.0 software from the GSEA Broad Institute website to carry out the Gene Set Enrichment Analysis (Subramanian et al., 2005) on custom pathway, including NOTCH signaling and hypoxia pathways (Harris, 2002), both from GSEA Broad Institute databases, and HSC pathways from published literatures (Eppert et al., 2011; Laurenti et al., 2013). Genes were

ranked based on the direction of the fold change $[\pm 1 \times -(log_{10}(pvalue))]$. The minimum and maximum number of genes in each pathway allowed for the GSEA was set to 15 and 1,000 respectively. FDR q-values were estimated to correct the p-values for testing multiple pathways. For each pathway, using the leading edge genes determined by a combination of the ranking and Enrichment Score (ES), we created a heatmap using the pheatmap R package (Kolde, 2012) to visualize the expression patterns between the groups compared. Prior to creating the heatmaps, gene expression values for the leading edge genes in each pathway were transformed using the rlog function in the DESeq2 R package (Love et al., 2014). In addition, the removeBatchEffect function in the Limma R package was used to remove subject specific effects accounting for the paired experimental design.

ImageStream

Human CD34+ cells were cultured in normoxia or hypoxia in vessels coated with DXI at 10 µg/mL in normoxia and 5 µg/mL in hypoxia. After overnight incubation, cells were collected and replated onto DXI coated plates for 1 hour. Following this brief exposure, cells were fixed in equal volumes of Cytofix (BD Biosciences) for 10 minutes at 37°C. Next, cells were permeabilized for 30 minutes at 4°C in Perm Buffer III (BD Biosciences). All fixed and permeabilized cells were incubated overnight in either anti-human activated NOTCH1 (Abcam, ab8925) or anti-human activated NOTCH2 (Sigma, SAB4502022) (both primary antibodies applied at a dilution factor of 1:100). The next day, cells were washed 3 times and then incubated in anti-rabbit IgG (H+L) antibodies conjugated to Alexa488 (1:300) (Sigma, SAB4600045) for 60 minutes at 4°C. Labeled cells were next stained with anti-human CD34 antibodies conjugated to allophycocyanin (1:5) (BD Pharmingen) for 30 minutes at 4°C. Finally, cells were washed 3 times, with the second to last wash including DAPI to allow for visualization of the nuclei. All wash and staining buffers contained 2% FBS.

Using the Inspire data acquisition software (Amnis Inc.), images of 10,000 CD34+ cells were captured for each condition on channel 1 for brightfield, channel 2 for cleaved NOTCH

signaling events, channel 7 for DAPI, and on channel 11 for CD34-APC positive cells. Excitation of the samples was performed with 405 nm, 488 nm, 642 nm, 785 nm lasers, at power settings of 120 mW, 20 mW, 150 mW, and 4 mW, respectively. Data analysis was performed using the Ideas software (Amnis Inc.).

Immunocytochemistry and confocal microscopy

After 4 hours of exposure to DXI at optimized densities, cells were fixed for 15 minutes in 4% paraformaldehyde. Following fixation, cells were washed with PBS then permeabilized for 30 minutes with 0.1% Triton-X in PBS. Fixed and permeabilized cells were then blocked for 30 minutes in 5% BSA in PBS and an additional 60 minutes in 5% BSA supplemented with FAB fragments (Jackson Laboratory) at a 1:20 dilution. To assess protein-protein interaction, cells were incubated overnight at 4°C with anti-HIF-1α (1:75) (Novus Biological) and anti-human activated NOTCH1 antibody (Abcam, ab8925) applied at a dilution factor of 1:400. The next day, cells were washed with 1% BSA in PBS then incubated for 60 minutes in goat anti-rabbit and goat anti-mouse secondary antibodies (1:100) labeled with Alexa 647 (Invitrogen, A32733) and Alexa 555 (Invitrogen, A32727), respectively. All antibodies were diluted in 1% BSA in PBS. Finally, cells were washed to remove any unbound antibody, and a DAPI stain was added to the second to last wash step to allow for identification of the nuclei.

To visualize the potential protein-protein interaction of HIF-1α and the intracellular domain of NOTCH, stained samples were imaged on a Zeiss 780 Confocal Microscope. Twenty cells from each condition (i.e., Normoxia ± DXI or Hypoxia ± DXI) were imaged in high resolution. Captured images were then deconvolved using Huygens software, then analyzed in Imaris software. Masking based on positive cleaved NOTCH staining, colocalization defined as overlapping cleaved NOTCH and positive HIF-1α staining, was determined using Pearson's coefficient of correlation in the region of interest.

Single cell RNA sequencing and data analysis

Human CD34+ cells from one donor were cultured for 2 hours in the presence of cytokines (SCF, FLT3 and TPO) in vessels coated with DXI at 10 µg/mL in normoxia and 5 µg/mL in hypoxia. Each condition was prepared in duplicates. After 2 hours, cells were harvested and immediately moved to single-cell RNA (scRNA) library preparation. scRNA libraries were prepared using the Drop-seq method. For full protocol details, refer to http://mccarrolllab.org/dropseq/. Single cells were resuspended at 1.0 x 10^5 cells/mL and encapsulated with barcoded Bead SeqB microparticles (Chemgenes) into droplets containing lysis buffer using a PDMS microfluidic device (FlowJem), aiming at capturing 3000-4000 single cells per technical replicate of each culture condition, two technical replicates were run per culture condition. Following single-cell encapsulation, droplet breakage, reverse transcription, exonuclease I treatment and PCR amplification were all performed following the standard Drop-seq protocol. The amplified cDNA and sequencing libraries were quantified using the Qubit dsDNA High Sensitivity assay (Thermo Fisher Scientific) and sized using a DNA High-sensitivity BioAnalyzer 2100 kit and instrument (Agilent Technologies). Sequencing libraries were prepared using the Nextera XT DNA sample prep kit (Illumina). The libraries were sequenced on the Illumina HiSeq 3000, with a read length of 20 bp of Read 1 using a custom primer (5' GCCTGTCCGCGGAAGCAGTGGTATCAACGCAGAGTAC 3'), 60 bp of Read 2, and 8 bp of index read 1 for sample demultiplexing. Sequencing depth was at least 50,000 raw read pairs per cell.

De-multiplexed scRNA-seq fastq files were processed using Drop-seq Tools v1.12. Read alignment and generation of the digital gene expression matrix were performed using STAR v2.5.4a with default settings and drop-seq-tools-1.12 in NIH Helix/Biowulf High Performing Computation (HPC) system. From read 1, 5' bases 1–12 and bases 13–20 with equal or higher than 10 quality score were tagged as cell barcode and unique molecular identifier (UMI), respectively, and then filtered for sequence alignment. Adapter sequence and poly-A tail sequence contamination were removed before sequence alignment. Data reads were aligned to the human reference genome hg19.

We used R language within the RStudio IDE throughout our analysis. The digital gene expression matrices for all samples were analyzed using Seurat version 3.2.0 (Butler et al., 2018). Quality control was performed to filter low-quality cells by retaining cells that had more than 500 genes and less than 5% of mapped reads mapping to mitochondrial genes. Gene expression values were normalized using Seurat's scTransform to account for technical variation in RNA recovery and sequencing depth. The filtered and normalized datasets were integrated via Seurat. To decrease noise and make downstream computations more tractable, the data were dimensionally reduced by projection onto the top 20 principal components. For clustering and visualization, the data were further dimensionally reduced to two dimensions via Uniform Manifold Approximation and Projection (UMAP), a non-linear dimensional reduction technique founded on the assumptions that the data is uniformly distributed on a connected Riemannian manifold with locally constant metric.

HSC and progenitor clusters were annotated by computing module scores of previously reported HSPC gene set (Eppert et al., 2011; Laurenti et al., 2013) using a previously described approach (Butler et al., 2018; Tirosh et al., 2016). We assigned each cluster a specific HSPC identity by statistically comparing module scores and assigning the top-scoring cell type to each cluster. In this manner, we annotated four clusters, including HSC, MEP, GMP and CLP clusters. We also confirmed expression levels of lineage defining genes within these clusters: HES1 (Yu et al., 2006), EGR1 (Min et al., 2008) and JUNB (Passegue et al., 2004) expression in the HSC cluster; MPO (Pellin et al., 2019) expression in the GMP cluster; GATA1 (Dore and Crispino, 2011) and ITGA2B (Pellin et al., 2019) expression in the MEP cluster; and DNTT and NPTX2 (Pellin et al., 2019) expression in the CLP cluster. The LMPP cluster was annotated by being enriched in the progenitor (most notably lymphoid) libraries and scoring higher in LTR-HSC signature than other progenitor clusters, but lacking expression of other specific lineage markers as defined. The MPP cluster was annotated by being enriched in the progenitor libraries and

scoring higher in LTR-HSC signatures than other progenitor clusters, but lacking expression of specific lineage markers as defined.

During hematopoiesis, cells transition between cell states asynchronously and towards different mature cell types (Qiu et al., 2017). We used Monocle version 3 to reconstruct differentiation trajectories for hematopoietic stem and progenitor cells based on their expression patterns of highly variable genes (Trapnell et al., 2014).

Differential gene expression analysis was performed within the HSC cluster using 2 methods as reciprocal validation: Wilcoxon rank sum test and DESeq2. Features with natural log fold change > 1 or < -1 for Wilcoxon rank sum test and > 0.25 or < -0.25 for DESeq2 as well as Bonferroni-adjusted p-value < 5% were declared as genome-wide significant. Overlap between the two differentially expressed gene lists was used for further analysis.

We used GSEA v4.1.0 software from the GSEA Broad Institute website to carry out GSEA on gene ontology (GO) molecular function gene sets as well as hallmark gene sets, both available in the Broad Institute Molecular Signatures Database (Subramanian et al., 2005). Genes were ranked based on the direction of the fold change $\left[\pm 1 \times -\left(log_{10}(pvalue)\right)\right]$ calculated by Wilcoxon rank sum test. The minimum and maximum number of genes in each pathway allowed for the GSEA was set to 15 and 1000 respectively. FDR q-values were estimated to correct the p-values for testing multiple pathways.

Data availability

The data generated for this study have been deposited at the Gene Expression Omnibus under accession codes GSE157465 and GSE157321.

Supplemental Figures

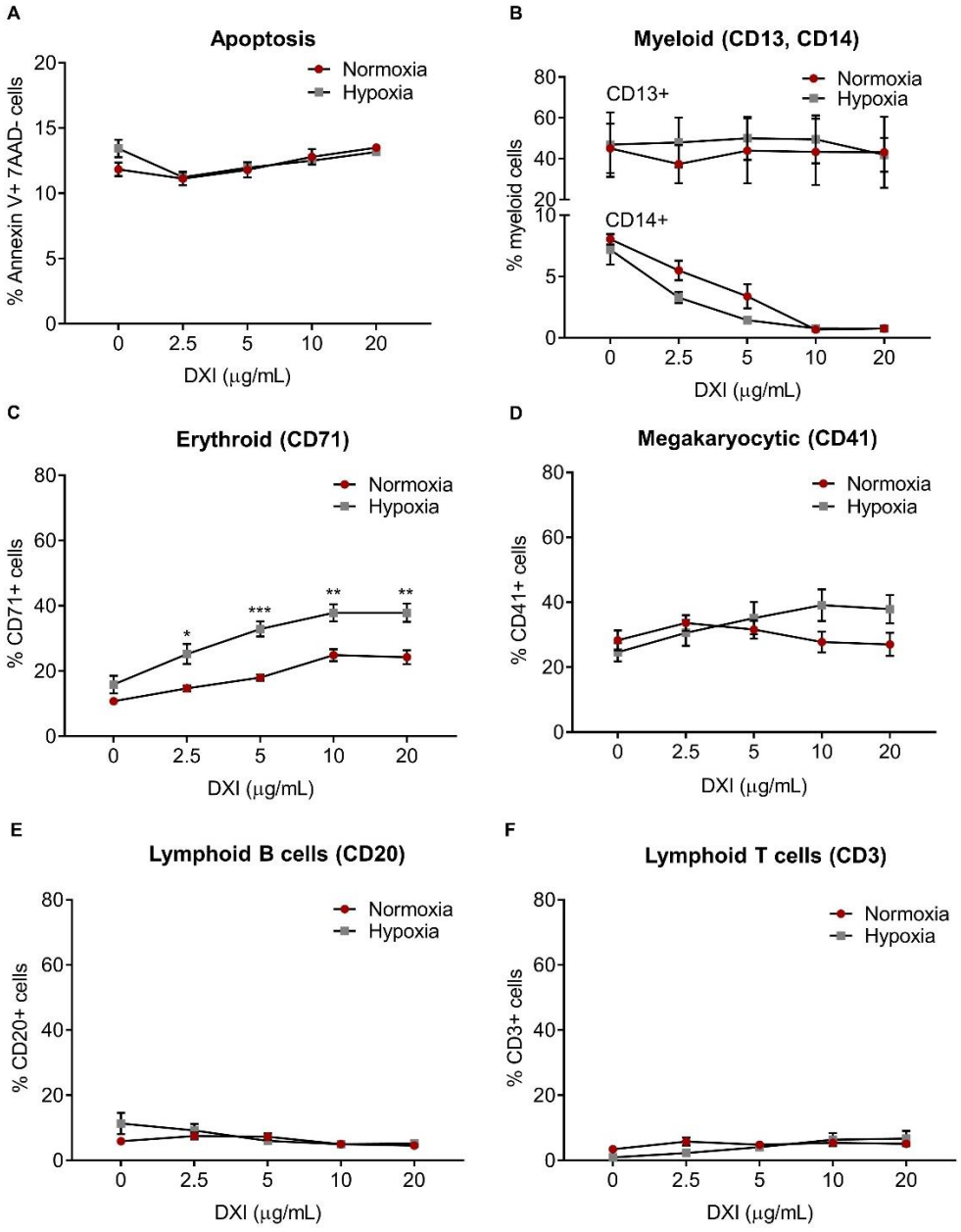

Figure S1 | Concurrent activation of NOTCH and hypoxia pathways in human CD34+ cells has minimal impact on cell survival or lineage differentiation. Human CD34+ cells were cultured under normoxia (21% O_2) or hypoxia (1-2% O_2) in vessels coated with fibronectin alone or combined with increasing concentrations of DXI (2.5, 5, 10 and 20 µg/mL). After 21 days in culture, cells were counted and characterized by flow cytometry. (A) Percentages of apoptotic cells in the CD34+ cell compartment (n = 3 independent donors). (B – F) Percentages of CD13+ or CD14+ myeloid cells (B), CD71+ erythroid cells (C), CD41+ megakaryocytic cells (D), CD20+ B cells (E) and CD3+ T-cells (F) (n = 3-5 independent donors). Data are displayed as mean ± SEM. Two-way ANOVA was used. * $p \leq 0.05$, ** $p \leq 0.01$, *** $p \leq 0.001$. Associated with Figure 1A.

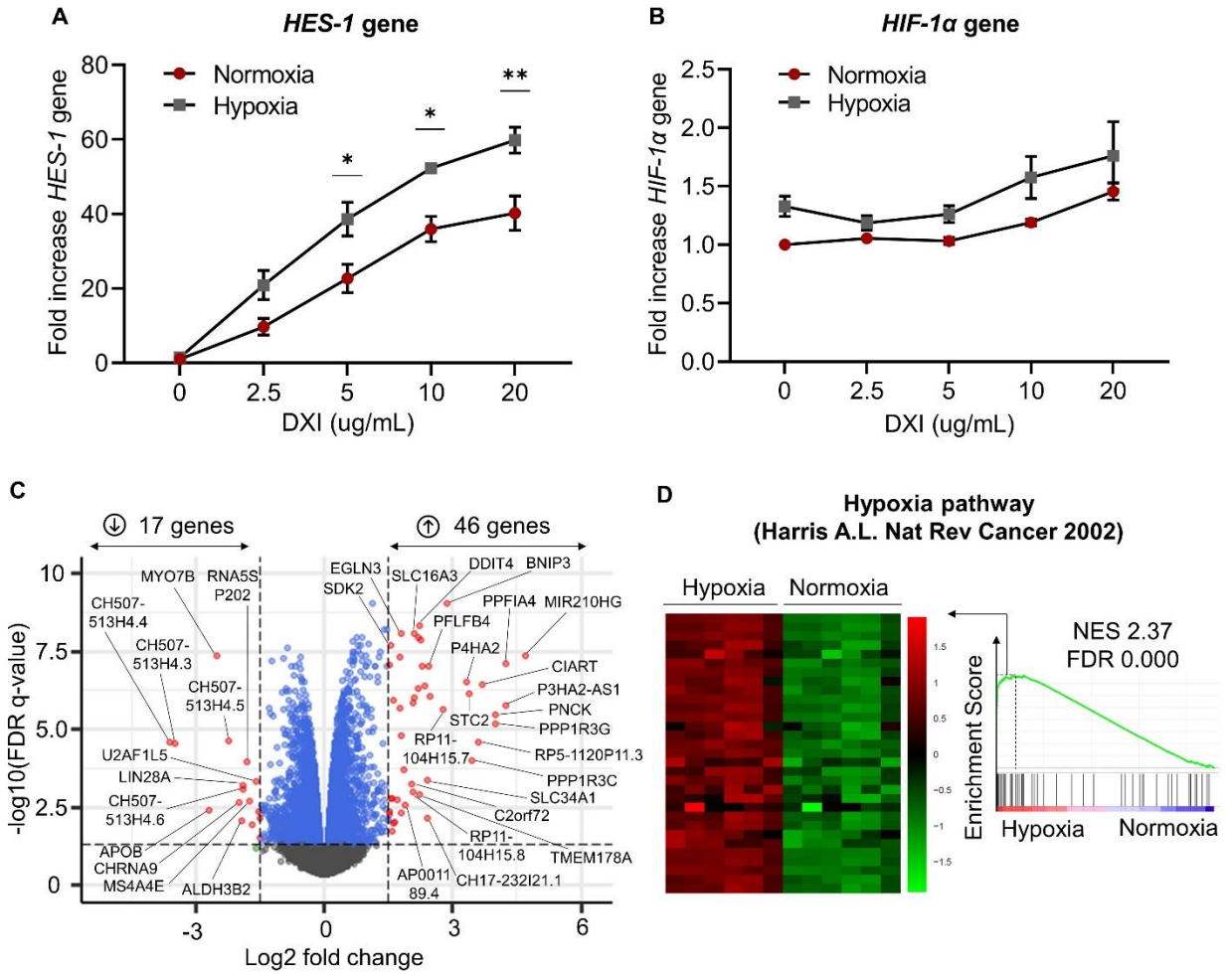

Figure S2 | Transcriptomic analysis of CD34+ cells treated with DXI in normoxic or hypoxic cultures. Transcriptomic analysis was performed on human CD34+ cells cultured for 24 hours in normoxia (21% O_2) or hypoxia (1-2% O_2) in vessels coated with optimized densities of DXI (10 µg/mL in normoxia; 5 µg/mL in hypoxia). (A) Comparison of *HES-1* gene expression between normoxic and hypoxic culture conditions, as measured by qRT-PCR (n = 9 technical replicates, from 3 independent donors). (B) Comparison of HIF-1α gene expression between normoxic and hypoxic culture conditions, as measured by qRT-PCR (n = 9 technical replicates, from 3 independent donors). (C) Volcano plot of differentially expressed genes in CD34+ cells cultured in hypoxia relative to normoxia. The x-axis corresponds to the log (base 2) of the fold change difference between groups and the y-axis corresponds to the negative log (base 10) of the false discovery rate (FDR) q-values. (D) Heatmap of leading edge subset (left) and enrichment plot (right) showing relative expression of genes associated with the hypoxia pathway. NES, normalized enrichment score. In panels A and B, data are displayed as mean ± SEM. Two-way ANOVA was used. * $p \leq 0.05$, ** $p \leq 0.01$. Associated with Figure 2A, Table S1 (panel C) and Table S2 (panel D).

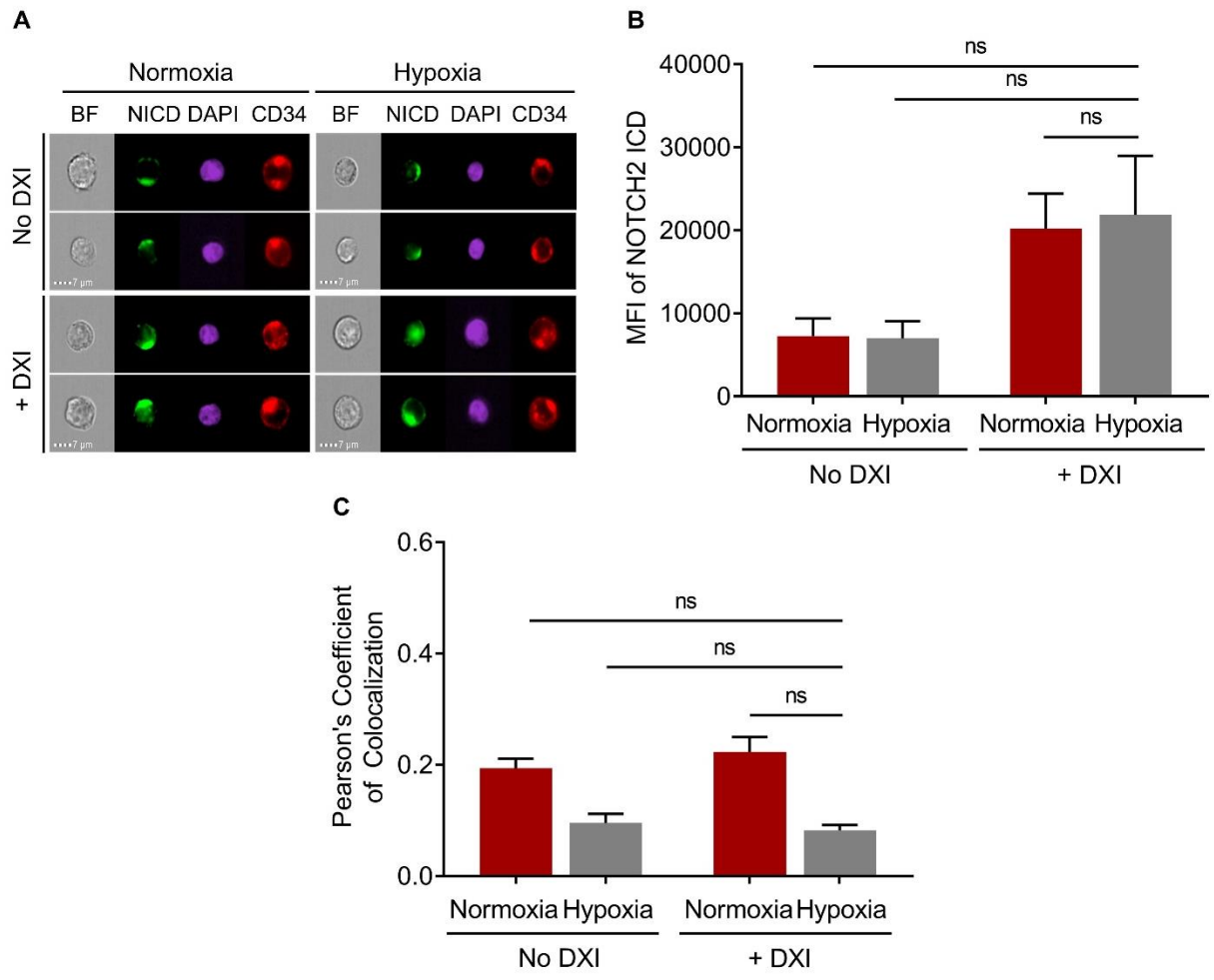

Figure S3 | Hypoxia does not affect signaling mediated by the intracellular domain of NOTCH2. (A) Representative ImageStream® images of human CD34+ cells cultured under normoxic or hypoxic conditions in the absence or with previously optimized concentrations of DXI. BF, bright field; NICD, NOTCH2 intracellular domain; DAPI, 4′,6-diamidino-2-phenylindole. (B) Quantification of the mean fluorescence intensity (MFI) of the intracellular domain (ICD) of NOTCH2 in 10,000 cells/condition. (C) Quantification of NOTCH2 ICD and HIF-1α signal colocalization in individual cells for each condition by the Pearson's correlation coefficient (n = 20 cells/condition). In panels B and C, data are displayed as mean ± SEM. One-sided (panel B) and two-sided (panel C) unpaired t-test were used. ns, not significant. Associated with Figure 2C, D (panels A and B) and Figure 2E, F (panel C).

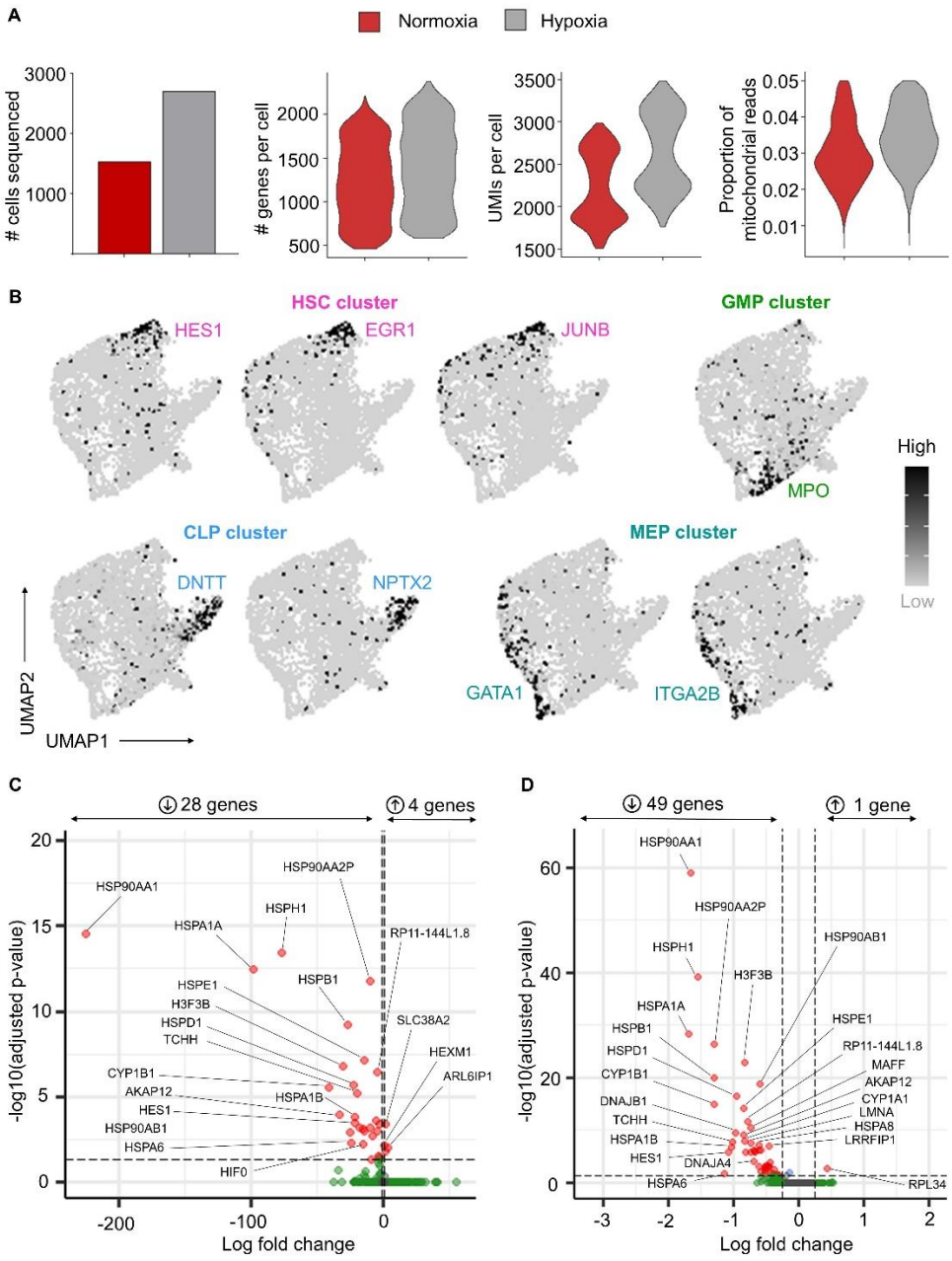

Figure S4 | Single cell RNA sequencing analysis of CD34+ cells treated with optimized DXI densities under normoxic or hypoxic conditions. (A) Total number of cells sequenced, and gene, transcript (Unique Molecular Identifiers, UMIs) and mitochondrial read counts per cell after quality control. (B) Representative gene expression maps of lineage defining gene signatures, including HES1, EGR1 and JUNB (hematopoietic stem cell [HSC] cluster); MPO (granulocyte-monocyte progenitor [GMP] cluster); DNTT and NPTX2 (common lymphoid progenitor [CLP] cluster); GATA1 and ITGA2B (megakaryocytic-erythroid progenitor [MEP] cluster). (C, D) Volcano plots of differentially expressed genes within the HSC cluster, analyzed by 2 methods for reciprocal validation: Wilcoxon rank sum test (C) and DESeq2 (D). The x-axis corresponds to the natural log of the fold change difference between groups and the y-axis corresponds to the negative log (base 10) of the adjusted p-values. Associated with Figure 4, Table S3 (panel C) and Table S4 (panel D).

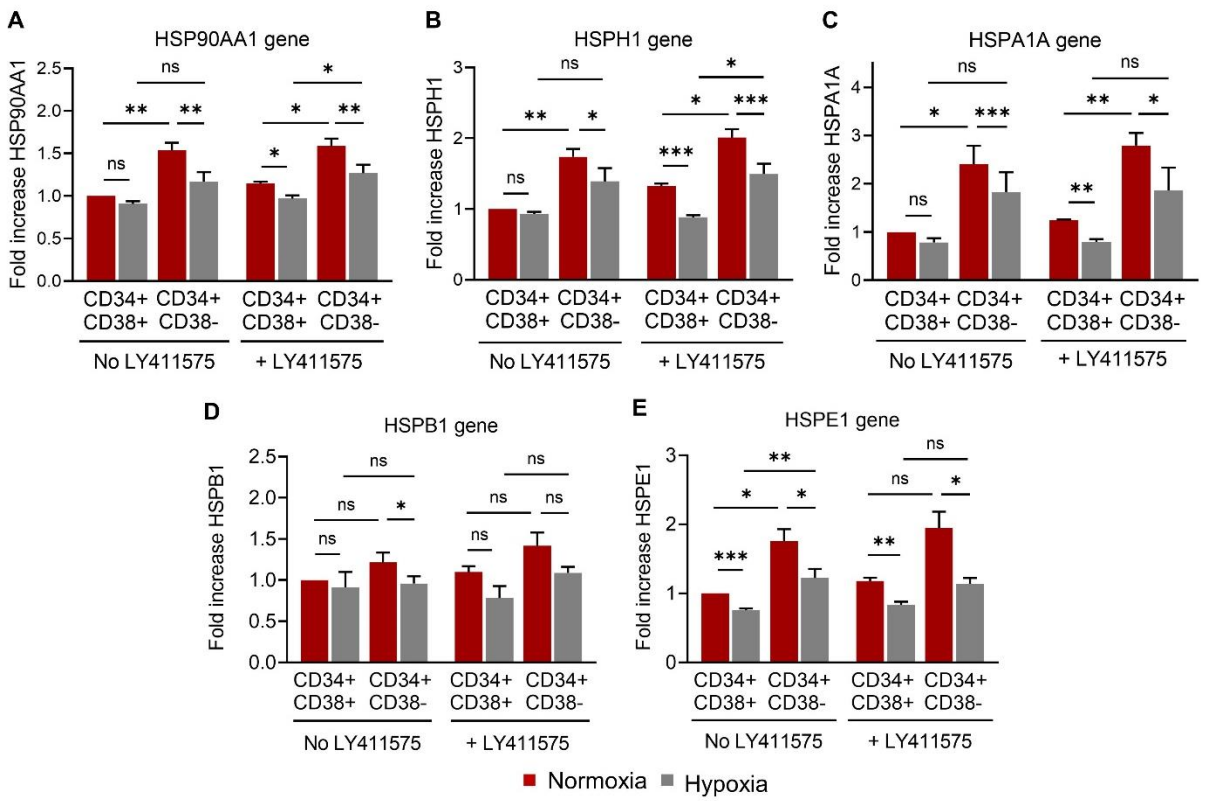

Figure S5 | Downregulation of ER stress response gene expression by hypoxia during DXI-mediated expansion of human long-term repopulating HSCs. (A-E) Validation of scRNA-seq data by qRT-PCR of the top differentially expressed ER stress response genes from human CD34+CD38+ hematopoietic progenitors and LTR-HSC-enriched CD34+CD38- cell populations after treatment with optimized DXI densities under normoxic or hypoxic conditions (n = 6 technical replicates, from 2 independent donors). Cells from each culture condition were incubated in the presence or absence of 10 μM LY411575, a small molecule inhibitor of γ-secretase-mediated proteolytic cleavage of NOTCH ICD. Blockade of NOTCH ICD cleavage and release by LY411575 did not reverse downregulation of ER stress response mediated by hypoxia during *ex vivo* culture with DXI. Data are displayed as mean ± SEM. One-way repeated measures ANOVA was used. * $p \leq 0.05$, ** $p \leq 0.01$, *** $p \leq 0.001$, ns, not significant. Associated with Figure 4D.

References

Bioinformatics, B. (2015). A Quality Control Tool for High Throughput Sequence Data

Butler, A., Hoffman, P., Smibert, P., Papalexi, E., and Satija, R. (2018). Integrating single-cell transcriptomic data across different conditions, technologies, and species. Nat Biotechnol *36*, 411-420.

Cipolleschi, M.G., Dello Sbarba, P., and Olivotto, M. (1993). The role of hypoxia in the maintenance of hematopoietic stem cells. Blood *82*, 2031-2037.

Danet, G.H., Pan, Y., Luongo, J.L., Bonnet, D.A., and Simon, M.C. (2003). Expansion of human SCID-repopulating cells under hypoxic conditions. J Clin Invest *112*, 126-135.

Delaney, C., Heimfeld, S., Brashem-Stein, C., Voorhies, H., Manger, R.L., and Bernstein, I.D. (2010). Notch-mediated expansion of human cord blood progenitor cells capable of rapid myeloid reconstitution. Nature medicine *16*, 232-236.

Delaney, C., Varnum-Finney, B., Aoyama, K., Brashem-Stein, C., and Bernstein, I.D. (2005). Dose-dependent effects of the Notch ligand Delta1 on ex vivo differentiation and in vivo marrow repopulating ability of cord blood cells. Blood *106*, 2693-2699.

Dore, L.C., and Crispino, J.D. (2011). Transcription factor networks in erythroid cell and megakaryocyte development. Blood *118*, 231-239.

Eppert, K., Takenaka, K., Lechman, E.R., Waldron, L., Nilsson, B., van Galen, P., Metzeler, K.H., Poeppl, A., Ling, V., Beyene, J.*, et al.* (2011). Stem cell gene expression programs influence clinical outcome in human leukemia. Nat Med *17*, 1086-1093.

Harris, A.L. (2002). Hypoxia--a key regulatory factor in tumour growth. Nat Rev Cancer *2*, 38-47.

Harrow, J., Frankish, A., Gonzalez, J.M., Tapanari, E., Diekhans, M., Kokocinski, F., Aken, B.L., Barrell, D., Zadissa, A., Searle, S.*, et al.* (2012). GENCODE: the reference human genome annotation for The ENCODE Project. Genome Res *22*, 1760-1774.

Hu, Y., and Smyth, G.K. (2009). ELDA: extreme limiting dilution analysis for comparing depleted and enriched populations in stem cell and other assays. J Immunol Methods *347*, 70-78.

Kim, D., Paggi, J.M., Park, C., Bennett, C., and Salzberg, S.L. (2019). Graph-based genome alignment and genotyping with HISAT2 and HISAT-genotype. Nat Biotechnol *37*, 907-915.

Kolde, R. (2012). Pheatmap: pretty heatmaps. R Package Version 61, 1–7 (Pheatmap: pretty heatmaps. R Package Version 61, 1–7).

Laurenti, E., Doulatov, S., Zandi, S., Plumb, I., Chen, J., April, C., Fan, J.B., and Dick, J.E. (2013). The transcriptional architecture of early human hematopoiesis identifies multilevel control of lymphoid commitment. Nat Immunol *14*, 756-763.

Law, C.W., Chen, Y., Shi, W., and Smyth, G.K. (2014). voom: Precision weights unlock linear model analysis tools for RNA-seq read counts. Genome Biol *15*, R29.

Liao, Y., Smyth, G.K., and Shi, W. (2014). featureCounts: an efficient general purpose program for assigning sequence reads to genomic features. Bioinformatics *30*, 923-930.

Love, M.I., Huber, W., and Anders, S. (2014). Moderated estimation of fold change and dispersion for RNA-seq data with DESeq2. Genome Biol *15*, 550.

Madar, V., and Batista, S. (2016). FastLSU: a more practical approach for the Benjamini-Hochberg FDR controlling procedure for huge-scale testing problems. Bioinformatics *32*, 1716-1723.

Min, I.M., Pietramaggiori, G., Kim, F.S., Passegue, E., Stevenson, K.E., and Wagers, A.J. (2008). The transcription factor EGR1 controls both the proliferation and localization of hematopoietic stem cells. Cell Stem Cell *2*, 380-391.

Passegue, E., Wagner, E.F., and Weissman, I.L. (2004). JunB deficiency leads to a myeloproliferative disorder arising from hematopoietic stem cells. Cell *119*, 431-443.

Pellin, D., Loperfido, M., Baricordi, C., Wolock, S.L., Montepeloso, A., Weinberg, O.K., Biffi, A., Klein, A.M., and Biasco, L. (2019). A comprehensive single cell transcriptional landscape of human hematopoietic progenitors. Nat Commun *10*, 2395.

Qiu, X., Mao, Q., Tang, Y., Wang, L., Chawla, R., Pliner, H.A., and Trapnell, C. (2017). Reversed graph embedding resolves complex single-cell trajectories. Nat Methods *14*, 979-982.
QUBES (2015). FastQC.
Ritchie, M.E., Phipson, B., Wu, D., Hu, Y., Law, C.W., Shi, W., and Smyth, G.K. (2015). limma powers differential expression analyses for RNA-sequencing and microarray studies. Nucleic Acids Res *43*, e47.
Robinson, M.D., and Oshlack, A. (2010). A scaling normalization method for differential expression analysis of RNA-seq data. Genome Biol *11*, R25.
Smyth G.K., G.R., Carey V.J., Huber W., Irizarry R.A., Dudoit S. (2005). limma: Linear Models for Microarray Data. In Bioinformatics and Computational Biology Solutions Using R and Bioconductor (Springer, New York, NY), pp. 397-420.
Subramanian, A., Tamayo, P., Mootha, V.K., Mukherjee, S., Ebert, B.L., Gillette, M.A., Paulovich, A., Pomeroy, S.L., Golub, T.R., Lander, E.S.*, et al.* (2005). Gene set enrichment analysis: a knowledge-based approach for interpreting genome-wide expression profiles. Proc Natl Acad Sci U S A *102*, 15545-15550.
Tirosh, I., Izar, B., Prakadan, S.M., Wadsworth, M.H., 2nd, Treacy, D., Trombetta, J.J., Rotem, A., Rodman, C., Lian, C., Murphy, G.*, et al.* (2016). Dissecting the multicellular ecosystem of metastatic melanoma by single-cell RNA-seq. Science *352*, 189-196.
Trapnell, C., Cacchiarelli, D., Grimsby, J., Pokharel, P., Li, S., Morse, M., Lennon, N.J., Livak, K.J., Mikkelsen, T.S., and Rinn, J.L. (2014). The dynamics and regulators of cell fate decisions are revealed by pseudotemporal ordering of single cells. Nat Biotechnol *32*, 381-386.
Uchida, N., Hsieh, M.M., Hayakawa, J., Madison, C., Washington, K.N., and Tisdale, J.F. (2011). Optimal conditions for lentiviral transduction of engrafting human CD34+ cells. Gene Ther *18*, 1078-1086.
Yan, Q., Bartz, S., Mao, M., Li, L., and Kaelin, W.G., Jr. (2007). The hypoxia-inducible factor 2alpha N-terminal and C-terminal transactivation domains cooperate to promote renal tumorigenesis in vivo. Mol Cell Biol *27*, 2092-2102.
Yu, X.B., Alder, J.K., Chun, J.H., Friedman, A.D., Heimfeld, S., Cheng, L.Z., and Civin, C.I. (2006). HES1 inhibits cycling of hematopoietic progenitor cells via DNA binding. Stem Cells *24*, 876-888.